ON NEAR-FIELD EFFECTS IN SIGNAL BASED ACOUSTIC EMISSION ANALYSIS

GEDANKEN ZU NAHFELDEFFEKTEN BEI DER SIGNAL-BASIERTEN SCHALLEMISSIONSANALYSE

DES EFFETS DE LA METHODE DU CHAMP ROCHE DANS DES SIGNALS DES EMISSIONS ACOUSTIQUES

Finck, Florian & Manthei, Gerd

SUMMARY

Transient elastic waves emitted by sudden failure within a specimen comprise information about the global stress field, processes in the sources, and effects of wave propagation in the medium. Signal based acoustic emission (AE) analysis allows for a comprehensive investigation of the alteration of the material, and fracture processes as AE sources. The mechanism of an AE source can be evaluated by the seismic moment tensor concept. This concept describes an AE source by a system of equivalent body forces. To handle such a complex problem, various assumptions are made in practice. One important assumption is the point source approximation. An AE source can be considered as a point source if both the distance of the sensor from the source and the wavelength of the signals are much greater than the linear dimension of the source. These requirements are fulfilled in case of a short duration of the source-time function observed in greater distance from the source. Since in AE measurements the wave field is often observed in smaller distances, near-field effects can occur. In the following, near-field effects are discussed analytically.

ZUSAMMENFASSUNG

Transiente, elastische Wellen, die durch Bruchprozesse in einem Probekörper ausgesendet werden, enthalten eine Vielzahl von Informationen über das globale Spannungsfeld, die Abläufe in der Bruchzone und Effekte des Wellenausbreitungsmediums. Mit Hilfe der signal-basierten Schallemissionsanalyse können Veränderungen der Materialeigenschaften beobachtet werden. Eine um-

fassende Untersuchung von Bruchmechanismen wird durch das Konzept des seismischen Momententensors möglich. Dabei wird die Schallemissionsquelle durch ein System äquivalenter Momente beschrieben. Um dieses äußerst komplexe, inverse Problem handhaben zu können, ist es nötig eine Reihe von Annahmen zu treffen. Eine wichtige Annahme ist die der Punktquelle. Eine Quelle kann als Punktquelle angesehen werden, wenn sowohl der Abstand zwischen Quelle und Empfänger, als auch die beobachtete Wellenlänge sehr groß gegen die räumliche Ausdehnung der Quellregion sind und die Quellzeitfunktion einem kurzem Puls ähnelt. Da bei der Schallemissionsanalyse das Wellenfeld häufig nur in geringem Abstand zur Quelle aufgezeichnet wird, muss mit Nahfeldeinflüssen gerechnet werden. Im folgenden Beitrag werden Nahfeldeffekte analytisch diskutiert.

RESUME

Des ondes elastiques qui ont emette d'une fracture dans une epreuve contenissent beaucoup d'informations sur la tension dans l'epreuve, sur le deroulement de la fracture et sur des effets visible dans la structure des ondes a cause de l'epreuve. Enregistrer tout le signal des emissions acoustiques on peut observer des changements dans le materiel. Des investigations globales devraient possible avec le brouillon du tensor du moment sismique. La source de l'emission acoustique est decrit d'un system des moment equivalent. La solution de cette probleme inverse est seulement possible avec quelques suppositions. Une supposition importante est que la source des ondes elastique est approxime d'un point. C'est possible quand la distance entre source et recepteur est grande par rapport a la region de source et quand la fonction qui decrit la source est une impulsion tres courte. A cause de la geometrie de l'epreuve la distance entre source et recepteur n'est pas toujour tres grande quand on enregistre des emissions acoustiques. Alors, il faut attendre a des derangements de la methode du champ roche. Dans ce quit suit les effets de la methode du champ roche devrai presente en detail.

KEYWORDS: acoustic emission, moment tensor, near-field

1. INTRODUCTION

Fracturing is a common and well-known procedure over a large range of scales. Knowledge about fracture processes helps to optimize the design of structures, to prevent accidents, and to understand the dynamics of seismic sources, e. g. earthquakes. Numerous methods applied in signal based acoustic emission analysis are related to seismological techniques. The observation of teleseismic events led to the accepted model of a *double-couple* mechanism as the origin of tectonic earthquakes. Typically, these are characterized by the relative slip movement of two tectonic plates, initiated in the so-called hypocenter. Meanwhile, a global network monitors earth seismicity and tectonic earthquakes in the far field and the source mechanisms are routinely determined using the moment tensors method [DZIEWONSKI et al., 1983]. The moment tensors give information about the seismic moment (magnitude), the orientation of the rupture plane, and the source type. The determination of the source type is important to identify explosions (e. g. nuclear tests) as well as for a detailed investigation of fracture processes [e. g. DAHLEN & TROMP, 1998]. Basic investigations in AE as well as material sciences are event counting and statistic analysis. Improved signal analysis (e.g. detection of the signal onset times and amplitudes) allows for a localization of the sources and the determination of source mechanisms using the moment tensor method. Various moment tensor inversion techniques were applied on AE data sets revealing plausible results for the stress field and failure mechanisms [e. g. OHTSU ET AL., 1991, GROSSE, 1996, MANTHEI ET AL., 2001, FINCK ET AL., 2003].

In most applications, the localization of AE events reveals a point in the coordinate system, or at least a solution which is very small compared to the wave length of the signal. Thereby, the point-source approximation appears for the first time. When analyzing the elastic wave field to gather information about source mechanisms the point source approximation is one important assumption. In practice all inversion techniques neglect near-field effects to simplify the algorithms. Often, the validity of this assumption was queried in the case of small-scale experiments in the laboratory. The development of a macro crack or a fault system is accompanied by a number of discrete fracturing events. BEN-ZION [2001] and STÖCKL & AUER [1976] published velocities of crack propagation in the order of the S-wave velocity in the respective medium. The extension of microcracks in rocks and therewith the source volume corresponds to the grain size in the material under quasi static loading conditions.

2. WHAT ARE NEAR-FIELD EFFECTS?

Two different approaches can be made to examine near-field effects. First, fracturing is a permanent deformation altering the material – a crack is opening or the crack surfaces are sliding along each other in a "short" period of time. The displacement in the source is characterized by non-linear effects which lead to a permanent offset in the signal. These effects vanish in great distances from the source and the signal can be described as linear-elastic wave. These non-linear effects are formulated as near-field and intermediate-field terms in seismology [e. g. AKI & RICHARDS, 2002, BEN-MENAHEM & SINGH, 1981].

Second, we take a closer look into that "short" period of time. According to the stress field and material properties, crack growth and development is also accompanied by phenomena like flaking, splitting, de-bonding, and friction during the slip of the crack surfaces. Also partial melting in the fracture zone can occur. Though these phenomena can be found over all scales, under the microscope as well as in the San Andreas fault system [e. g. EISBACHER, 1996], they are usually hidden for a direct observation and will not be investigated in this article. Anyway, these effects will contribute to the complexity of the registered signals, especially at high frequencies. It is obvious, that the point-source approximation ignores these phenomena, which are depending on time and space within the source.

3. ANALYTICAL DESCRIPTION OF THE WAVE FIELD

The concept of the moment tensor and its application on acoustic emission signals was already discussed in numerous publications [e. g. MANTHEI, 1991, GROSSE, 1999]. In these publications the evaluated AE sources were considered as point sources and near-field terms were neglected a priori.

Studying near-field effects, we will get into the problem at an advanced point. AKI & RICHARDS [2002] stated the initial point of our investigation with Eqn. 1. The moment tensor **M** is convoluted with simplified Green's functions **G** for a homogenous and isotropic full space. This equation describes the n^{th}-component of the displacement field. γ_i are the direction cosines of the senor position relative to the source location, r is the distance between source and receiver, α and β are the P- and S-wave velocities, respectively.

$$
\begin{aligned}
M_{pq} * G_{np,q} = & \left(\frac{15\gamma_n\gamma_p\gamma_q - 3\gamma_n\delta_{pq} - 3\gamma_p\delta_{nq} - 3\gamma_q\delta_{np}}{4\pi\rho} \right) \frac{1}{r^4} \int_{r/\alpha}^{r/\beta} \tau M_{pq}(t-\tau)\,d\tau \\
& + \left(\frac{6\gamma_n\gamma_p\gamma_q - \gamma_n\delta_{pq} - \gamma_p\delta_{nq} - \gamma_q\delta_{np}}{4\pi\rho\alpha^2} \right) \frac{1}{r^2} M_{pq}\left(t - \frac{r}{\alpha} \right) \\
& - \left(\frac{6\gamma_n\gamma_p\gamma_q - \gamma_n\delta_{pq} - \gamma_p\delta_{nq} - \gamma_q\delta_{np}}{4\pi\rho\beta^2} \right) \frac{1}{r^2} M_{pq}\left(t - \frac{r}{\beta} \right) \\
& + \frac{\gamma_n\gamma_p\gamma_q}{4\pi\rho\alpha^3} \frac{1}{r} \dot{M}_{pq}\left(t - \frac{r}{\alpha} \right) \\
& - \left(\frac{\gamma_n\gamma_p - \delta_{np}}{4\pi\rho\beta^3} \right) \gamma_q \frac{1}{r} \dot{M}_{pq}\left(t - \frac{r}{\beta} \right)
\end{aligned}
\tag{1}
$$

The first term of Eqn. 1 describes the near-field term which is proportional to $1/r^4$. The following terms describe the intermediate-field and the far-field of the P- and S-waves which are proportional to $1/r^2$ and $1/r$, respectively.

To calculate the Green's function according to Eqn. 1 we used a stepwise parabolic function (Eqn. 2) with a very short duration of only four samples (sampling interval is 100 ns which corresponds to 10 MHz) [KÜHNICKE, 1986]. The time derivation of this function is a triangular pulse, which gives "needle" pulses at times of the P-wave and the S-wave arrival.

$$
f_{pulse}(t) = \begin{cases} 0 & ;t < 0 \\ \dfrac{2t^2}{T_P{}^2} & ;t < T_P/2 \\ \dfrac{4t}{T_P} - \dfrac{2t^2}{T_P{}^2} - 1 & ;t > T_P/2 \\ 1 & ;t > T_P \end{cases}
\tag{2}
$$

Then we convolved the Green's functions with the wavelet representing the source-time function. We chose a wavelet proportional to $\ddot{f}(t)$ (Eqn. 3) described by [MÜLLER, 1987].

$$
\ddot{f}(t) = \sin\left(2\pi \, t/T_a \right) - 1/2 \sin\left(4\pi \, t/T_a \right)
\tag{3}
$$

This wavelet corresponds to the second time derivative of a step function with rise time T_a. Convolution of the Green's function with the first derivative

$\dot{f}(t)$ of the source-time function yields the displacement signal which is a pulse in the far field of the P- and S-waves. Fig. 1 shows the step function *f(t)* (continuous line) and its first and second time derivatives $\dot{f}(t)$ (dashed line) and $\ddot{f}(t)$ (dash-dotted line), respectively.

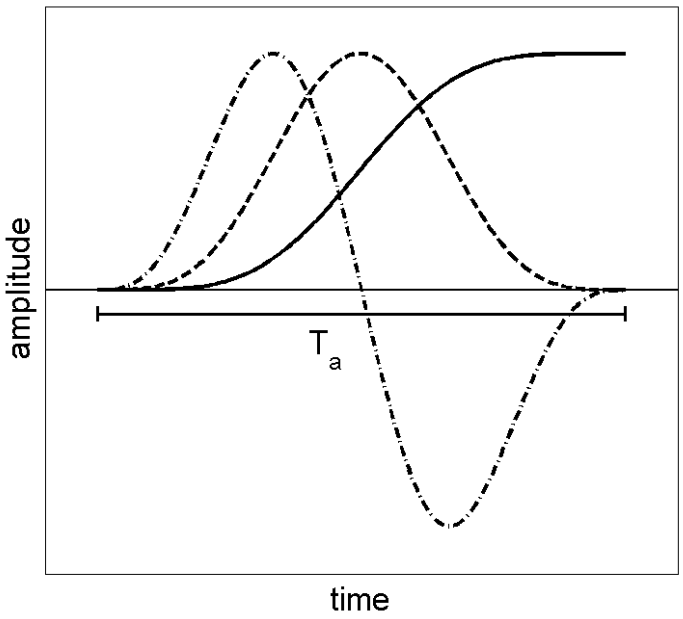

Fig. 1: Source-time function (continuous line) with rise time T_a and its first (dashed line) and second time derivatives (dash-dotted line) [MÜLLER,1987].

On the basis of Eqns. 1 to 3 a MATLAB® routine was developed to calculate synthetic seismograms. In this program the sensor position and its direction, the source mechanism (moment tensor), the rise time, and additional parameters concerning material properties can be entered.

4. RESULTS

The displacement field was studied with respect to source type, distance between source and receiver and duration of the source-time function. Furthermore, the influence of the sensor orientation was examined. In the following, various examples of synthetic calculations will be presented. An estimation of the influence of near-field and intermediate-field effects on the entire displacement is performed at the end of this section. The calculations are performed for an isotropic and homogeneous full space. P-wave velocity $\alpha = 4000$ m/s, S-wave velocity $\beta = \alpha/1.71$, and mass density $\rho = 2700$ kg/m^3 were used, as these parameters are typical for concrete.

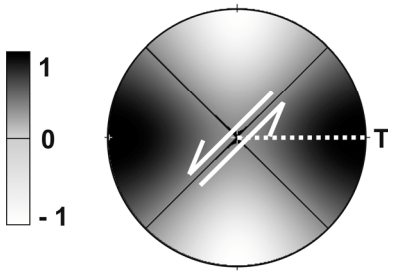

Fig. 2: Stereographic projection of the radiation pattern of a double-couple mechanism. Sinistral slip on one of the nodal planes is indicated by the arrows. The P-wave amplitude is maximal in direction of the T-axis.

Eqn. 1 yields a transient 3-dimensional wave field. To plot this field, a projection is useful to illustrate the effect of the three displacement terms. Fig. 3 shows the displacement signal of a double-couple (DC) mechanism (Fig. 2) in a distance of 0.2 m and a source-time duration of 10 µs. The displacement signal is decomposed into a radial P-wave component (left-hand side) and a horizontal polarized S-wave component (in the middle). The right-hand side of Fig. 3 displays the absolute amplitudes of the superposition of both wave types. Furthermore, the figures show the contribution of the near-field term (dash-dotted line), the intermediate-field term (dotted line), and finally the far-field term (dashed line). The observation was performed at an angle of $\varphi = 22.5°$ relative to the T-axis of the double-couple mechanism (see Fig. 2). In this direction no nodal plane occurs in the radiation pattern of the P- and S-wave.

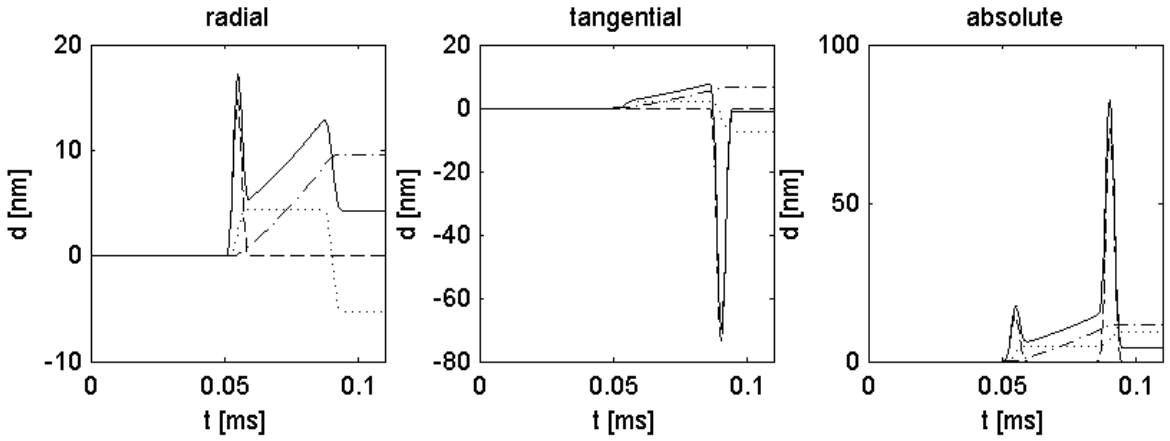

Fig.3: Far-field, intermediate-field and near-field terms of displacement signal in a distance of 0.2 m with source-time duration of 10 µs.

It can be seen, that the P-wave pulse occurs only in the radial (left-hand side of Fig. 3) and the S-wave pulse in the tangential direction (middle of Fig. 3). The right-hand side of Fig. 3 shows both wave types. The near-field and intermediate-field terms appear between the P- and S-wave pulses, which lead to a permanent signal offset after the S-wave pulse. The maximum amplitude of the S-wave measured at an angle of $\varphi = 45°$ is about 5 times of the maximum amplitude of the P-wave measured at an angel of $\varphi = 0°$.

Fig. 4 and Fig. 5 show the synthetic displacement and velocity signals, respectively, of a double-couple mechanism observed in distances of 0.1 m, 0.2 m,. and 0.3 m. Two values of the source-time duration T_a were used, 10 µs and 20 µs, which corresponds to typical frequencies of 100 kHz and 50 kHz observed in laboratory tests on concrete specimens. The radial component of the total displacement field is plotted as a continuous line and the radial component of the far-field term is plotted as a dashed line.

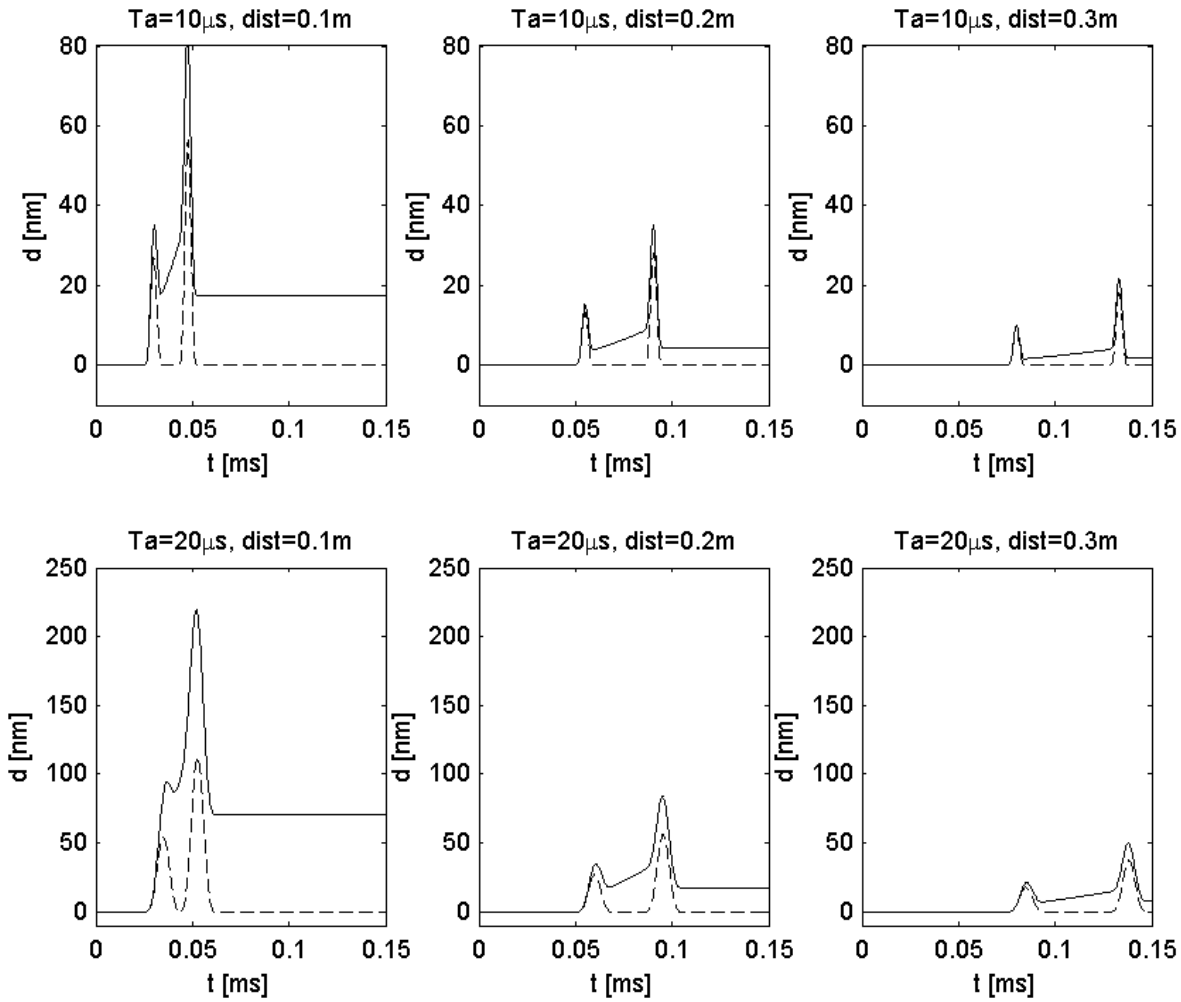

Fig. 4: Plot of calculated displacement signals for a point source in an infinite medium as received in various distances r from the source with source-time duration of 10 µs and 20 µs. Continuous lines show the complete displacement signal, dashed lines show only the far-field displacement signal. The pulses correspond to the P- and S-wave onsets, respectively.

The figures clearly illustrate the dependency of the signals with distance between source and receiver (from left to right) and with source-time duration. In a short distance the P-wave and S-wave pulses are overlapped, especially for a longer pulse duration (left-hand side of Fig. 4). The contribution of the near-field terms of the displacement signal is obvious at times between P- and S-wave arrivals. As the travel paths become longer or the pulse duration becomes

shorter the difference between the complete displacement and the far-field term alone becomes less apparent.

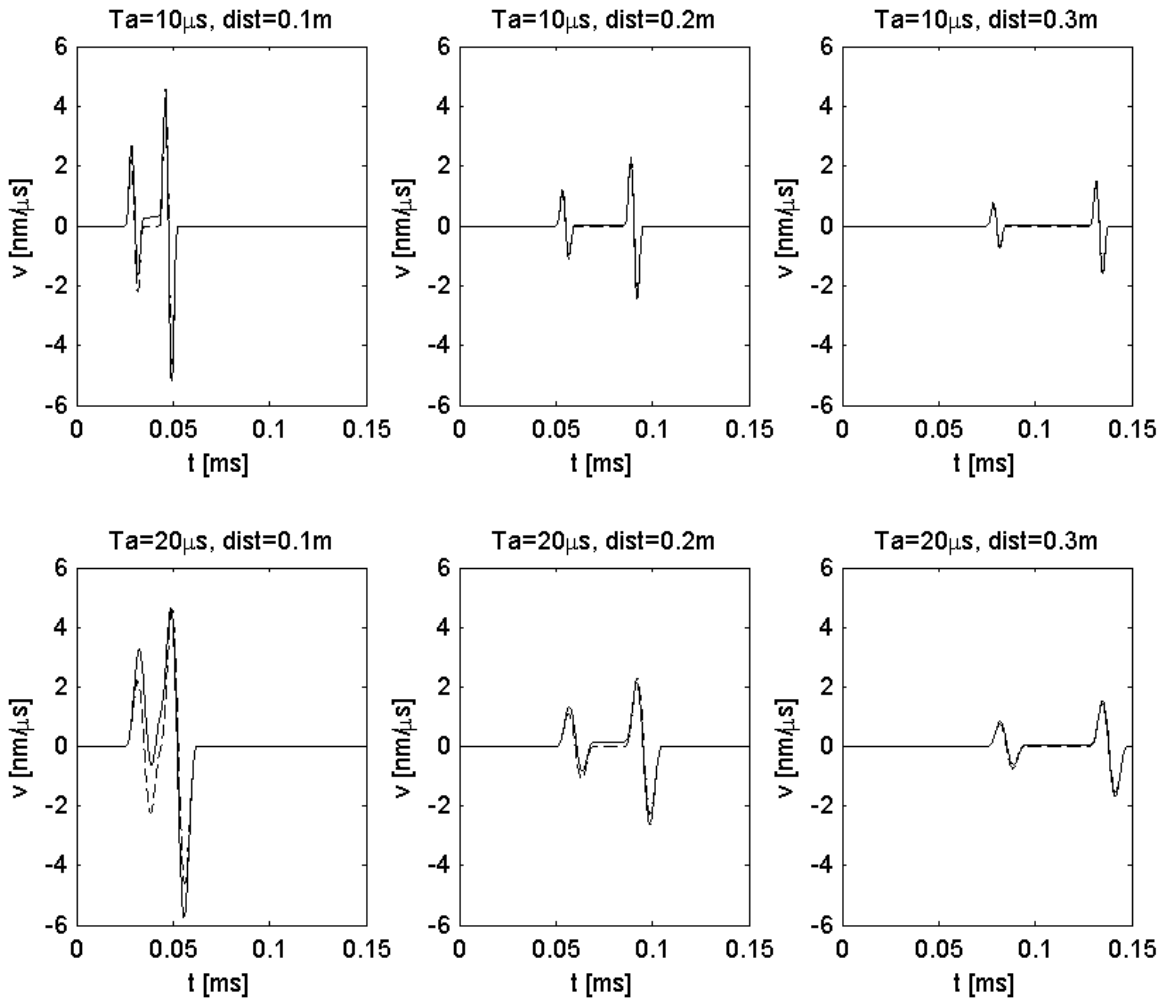

Fig.5: Same plot as Fig. 4 for velocity signal.

In the case of a velocity signal (Fig. 5), which is more realistic in AE, because broadband AE sensors are supposed to be a velocity sensor, the effect of the near-field terms significantly decreases.

On the basis of these calculations, we estimated a critical source-time duration τ_c as a function of rise time T_a. For source-time durations $\tau < \tau_c$ at distances $r < r_c$ (with $r = \alpha * \tau$ and $r_c = \alpha * \tau_c$) the influence of the near-field terms on the P-wave amplitudes was greater then 10%. In this case we assume that near-field effects can *not* be ignored in application of the moment tensor method. Fig. 6 shows the critical source-time duration τ_c versus rise time T_a for a pure double-couple mechanism and a pure tensile mechanism. In both calculations, the radial component at $\varphi = 0°$ was observed. A linear relation was obtained. According to these calculations, the near-field term can be ignored in the

case of a double-couple mechanism in distances greater than approximately 6 wavelengths of the P-wave. For a tensile crack (mode I), near-field effects are attenuated already after approximately 3.5 wavelengths of the P-wave. In the case of the double-couple, the position of the sensor relative to the source did not affect the results on the radial component, but for mode I a minor variation was observed.

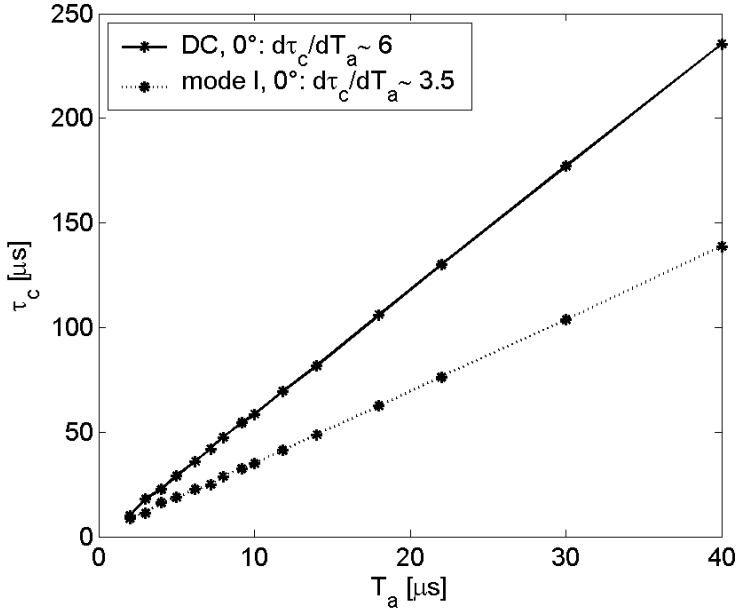

Fig. 6: Critical source-time duration τ_c versus rise time T_a for a pure double-couple mechanism (continuous line) and a pure tensile mechanism (dotted line) observed on the radial component and $\varphi = 0°$.

Fig. 2 shows that the near-field also has a transversal component. When the sensor is not oriented radial to the source, this has an additional consequence on the registered wave-field. To visualize this phenomenon, the number of wavelengths necessary for near-field effects to decrease under the 10% threshold was calculated as a function of the sensor position to the source as well as the relative orientation of the sensor to the source. Results are given as two matrices in Fig. 7, where the number *n* of wavelengths is coded due to a grayscale. On the x-axis, the angle σ is giving the orientation of the sensor to the vector from source to receiver. The calculation was performed for σ = -85° in steps of 10° to σ = 85°. On the y-axis, the angle φ is plotted from $\varphi = 0°$ to $\varphi = 180°$. The left image shows results for the double couple, the right image for a tensile crack.

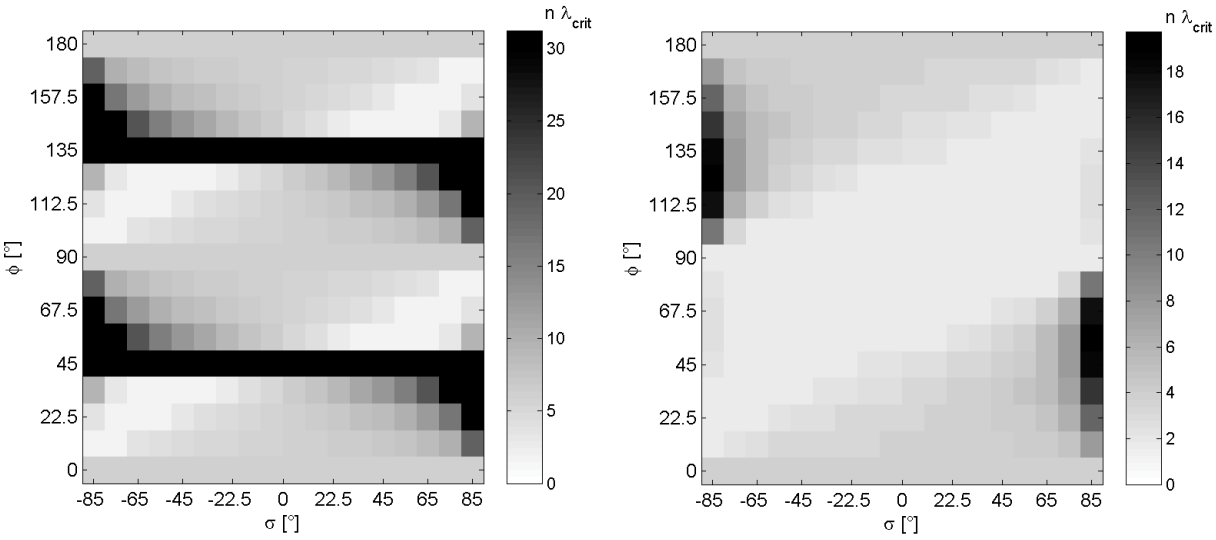

Fig. 7: Critical number of wavelengths as function of position and orientation of the sensor to the source for double-couple (left) and a pure tensile mechanism (mode I, right).

Depending on the orientation of the sensor, a decrease or an increase of disturbing near-field effects on the measured amplitudes is obtained. This is caused by an interference of near-field effects on the tangential and the radial component. In both figures, the symmetry of the matrices due to the radiation patterns of the source types is evident. In particular, close to the nodal planes of the double couple, where P-wave amplitudes are weak anyway, the registered data are highly influenced by near field effects.

5. CONCLUSION

Our investigations show, that near-field effects can not generally be neglected in signal based acoustic emission evaluations. A 10% residual is inherent for a pure double-couple mechanism below 100 kHz measured in distances smaller than 0.24 m in concrete. Also, the relative orientation of the sensor axis to the source and position of the sensor seems to affect the results. In the future, we will investigate the influence of near field effects on moment tensor inversion, also for mixed-mode source types. Furthermore, the influence of the sensor characteristic will be taken into account. First calculations show, that a high-pass filter with a corner frequency of approximately 30 kHz further reduces near-filed effects. Our piezoelectric transducers can be regarded as high-pass filters.

Concerning our results, the experimental set-up should be optimized. A three component registration would allow for the evaluation of a radial component, independent from the geometry of the specimen. To minimize the influ-

ence of near-field effects, normal incidence of the wave field on the sensors should be preferred.

ACKNOLEDGEMENTS

These investigations were partially founded by the Deutsche Forschungsgemeinschaft (DFG) within project SFB 381 and in close collaboration between IWB and *Gesellschaft für Materialprüfung und Geophysik mbH*, Obermörlen.

REFERENCES

[1] K. AKI & P. G. RICHARDS: Quantitative Seismology; 2nd Edition. University Science Books, CA Sausalito, 2002.

[2] A. BEN-MENAHEM, S. J. SINGH: Seismic Waves and Sources. Springer-Verlag, New York, 1981.

[3] Y. BEN-ZION: Short Course: *Introduction to Dynamics of Earthquakes and Faults.* Lecture notes, Institute of Geophysics, Munich, 2001.

[4] F. A. DAHLEN & J. TROMP: Theoretical Global Seismology. Princeton University Press, Princeton, New Jersey, 1998.

[5] A. M. DZIEWONSKI, J. H. WOODHOUSE: *An experiment in systematic study of global seismicity: centroid-moment solution for 201 moderate and large earthquakes.* J. Geophys. Res., Vol. 88, pp. 3247-3271, 1983.

[6] FINCK, M. YAMANOUCHI, H.-W. REINHARDT, C. U. GROSSE: *Evaluation of mode I failure of concrete in a splitting test using acoustic emission technique*. International Journal of Fracture, Vol. 124, pp. 139-152, 2003.

[7] G. H. EISBACHER: Einführung in die Tektonik, 2. Auflage. Enke Verlag, Stuttgart, 1996.

[8] C. U. GROSSE: *Quantitative zerstörungsfreie Prüfung von Baustoffen mittels Schallemissionsanalyse und Ultraschall*. Dissertation, Universität Stuttgart, 1996.

[9] C. U. GROSSE: *Grundlagen der Inversion des Momententensors zur Analyse von Schallemissionsquellen. Werkstoffe und Werkstoffprüfung im Bauwesen*. Festschrift zum 60. Geburtstag von Prof. Dr.-Ing. H.-W. Reinhardt, Libri BOD, Hamburg, pp. 82-105, 1999.

[10] H. KÜHNICKE: *Möglichkeiten zur Berechnung von Parametern der Quellenfunktionen aus den Aufnehmersignalen.* 6. Kolloquium Schallemission, Zittau, S. 18-20, 1986.

[11] G. MANTHEI: *Bestimmung des Typs und der Orientierung von Schallemissionsquellen in Salzgestein mit der Methode des Momententensors.* Diplomarbeit. Institut für angewandte Physik, Johann Wolfgang Goethe-Universität, Frankfurt. a. M., 1991.

[12] G. MANTHEI, J. EISENBLÄTTER, T. DAHM: *Moment tensor evaluation of acoustic emission sources in salt rock.* Construction and Building Materials, **15**, pp. 297-309, 2001.

[13] G. MÜLLER: *Inversion.* Vorlesungsskript, Johann Wolfgang Goethe-Universität, Frankfurt. a. M., 1987.

[14] M. OHTSU, M. SHIGEISHI, H. IWASE & W. KOYANAGI: *Determination of crack location, type and orientation in concrete structures by acoustic emission*. Magazine of Concrete Research, Vol. 43, No. 155, pp. 127-134, 1991.

[15] H. STÖCKL, F. AUER: *Dynamic Behavior of a tensile crack: finite difference simulation of fracture experiments*. Int. Journal of Fracture, Vol. 12, No. 3, pp. 345-358, 1976.